Colloids and Surfaces A 561 (2019) 201–208

Contents lists available at ScienceDirect

Colloids and Surfaces A

journal homepage: www.elsevier.com/locate/colsurfa

Micellization of a weakly charged surfactant in aqueous salt solution: Self-consistent field theory and experiments

Álvaro González García[a,b,c], Elizabeth Maria Timmers[c,d,e], Noah Romijn[a,b,c], Shidong Song[a,c], Sheen Sahebali[c], Remco Tuinier[a,b,c,*], Ilja Karina Voets[c,d,e,**]

[a] Laboratory of Physical Chemistry, Department of Chemical Engineering and Chemistry, Eindhoven University of Technology, P.O. Box 513, 5600 MB, Eindhoven, The Netherlands
[b] Van 't Hoff Laboratory for Physical and Colloid Chemistry, Department of Chemistry & Debye Institute for Nanomaterials Science, Utrecht University, Padualaan 8, 3584 CH Utrecht, The Netherlands
[c] Institute for Complex Molecular Systems, Eindhoven University of Technology, P.O. Box 513, 5600 MB, Eindhoven, The Netherlands
[d] Laboratory of Self-Organizing Soft Matter, Department of Chemical Engineering and Chemistry, Eindhoven University of Technology, P.O. Box 513, 5600 MB, Eindhoven, The Netherlands
[e] Laboratory of Macro-Organic Chemistry, Department of Chemical Engineering and Chemistry, Eindhoven University of Technology, P.O. Box 513, 5600 MB, Eindhoven, The Netherlands

GRAPHICAL ABSTRACT

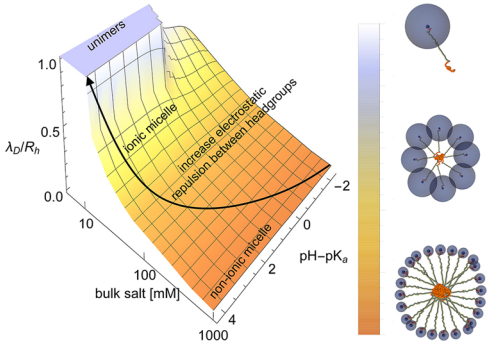

ARTICLE INFO

Keywords:
Surfactants
Self-assembly
Model systems

ABSTRACT

Self-consistent field (SCF) calculations and light scattering experiments were performed to study the pH and salt response of micelles composed of surfactants with a single weak acid group in aqueous salt solution. To this end, the common surfactant Brij 35 was oxidized to yield a polyoxyethylene alkyl ether carboxylic acid with a single terminal weakly charged carboxylic acid group in alkaline media. At low pH values, the micellar hydrodynamic radii (R_h) are independent of the salt concentration. By contrast, at pH values around the acid dissociation constant (pH ≈ pK$_a$ ± 1), the micellar radius decreases upon increasing pH until a salt-dependent plateau value is reached. The reduction in micellar size is more pronounced for lower salt concentrations. The SCF computations are in qualitative agreement with the experimental results and further reveal a limiting value for R_h corresponding approximately to the Debye length λ_D. Self-assembly into micelles is suppressed for low salt concentrations that would yield $R_h < \lambda_D$. Instead, the surfactants remain as unimers in solution. The results are

* Corresponding author at: Laboratory of Physical Chemistry, Department of Chemical Engineering and Chemistry, P.O. Box 513, 5600 MB, Eindhoven, The Netherlands.
** Corresponding author at: Laboratory of Self-Organizing Soft Matter, Department of Chemical Engineering and Chemistry, P.O. Box 513, 5600 MB, Eindhoven, The Netherlands.
E-mail addresses: r.tuinier@tue.nl (R. Tuinier), i.voets@tue.nl (I.K. Voets).

https://doi.org/10.1016/j.colsurfa.2018.10.039
Received 17 August 2018; Received in revised form 11 October 2018; Accepted 16 October 2018
Available online 17 October 2018

summarized in a state diagram displaying the preferred surfactant configuration in solution as a function of R_h/λ_D, pH and salt concentration.

1. Introduction

The self-association of charged surfactant molecules or polyelectrolytes in solution depends not only on their concentration and composition [1,2], but also on solution conditions such as temperature, pH [3–5], and bulk salt concentration [6–10]. The number and types of species present in solution [11–17] and their polydispersity also affect the final self-assembled structure [18]. The self-assembly of amphiphilic molecules into different morphologies (spherical, cylindrical, lamellar) has been reported in experimental [5,19], theoretical [2,8,20] and simulation [21,22] studies. Furthermore, depending both on the type of building blocks and the solvent conditions, complete phase separation (highly hydrophobic amphiphilic polymers) or dissolution (polyelectrolytes or surfactants) may be energetically more favorable than micro-phase separation [2,23,24]. Understanding the asssociation state of a polymer in solution is not only interesting from a fundamental perspective, but also for many industrial applications [25–27].

In this paper we focus on the self-organization of a weakly-charged (or annealed) surfactant in solution, as these compounds are widely present in detergents, antiseptics, emulsifiers, coatings and (de)foaming agents among other products [28,29]. For instance, Brij 35 is used as detergent for ion-exchange chromatography [30]. This surfactant is also regularly present in soaps, shampoos and dyes [31]. In this work, the self-assembly properties of a modified Brij 35 functionalized with a single acetic acid group are studied. This provides a simple model system for a low molar mass, amphiphilic, weakly-charged surfactant whose behavior in solution is expected to hold for other (weak) anionic and cationic surfactants. At pH-values far below the dissociation constant of the acid group (pK_a), the surfactant response in solution is expected to resemble that of non-ionic surfactants (such as Brij 35). On the contrary, when the acid gets deprotonated ($pH \gg pK_a$) the model surfactant shall recover the response of an ionic (or cationic) surfactant (such as SDS). This class of surfactants with tunable properties may be of interest for different applications [32]. For example, due to their mildness and resistance to hard water conditions and high temperatures (among other properties), they find applications as household and industrial cleaning agents [33]. Also, as these surfactants form stable emulsions in presence of cations, they are used for enhanced oil recovery [34]. Furthermore, their pH response may be of use for metal ion recovery [35].

In the present study we show how a relatively simple molecular approach employing the well-established Scheutjens-Fleer Self Consistent Field (SCF) model for self-assembly helps to explain the experimentally measured micelle size as a function of pH and salt. The SCF approach has been applied successfully to amphiphilic polyelectrolytes [24] and charged surfactants [8,20] in solution. To the best of our knowledge, no reports are available to date on SCF studies concerning the solution behavior of surfactants with a *single annealed* group. For this reason, we compare the experimentally measured properties of modified Brij 35 micelles in solution with the results arising from the SCF approach. The SCF calculations allow explaining the experimentally observed changes in micellar size with increasing pH in terms of increasing electrostatic repulsions between the carboxyl groups.

2. Materials and methods

2.1. Materials, sample preparation and experiments

The model system studied is a pH and charge-screening responsive glycolic acid ethoxylate lauryl ether (GAELE): a low molar mass amphiphile. The GAELE surfactant was obtained from commercially available Brij 35 via oxidation of the hydroxyl end group (hence, we refer to it as ModBrij 35 for simplicity; see Fig. 1). Chemicals were purchased from Sigma-Aldrich (Merck) and used as received. Nuclear magnetic resonance (NMR) data were recorded on a Bruker Advance-III 400 MHz equipped with a BBFO probe from Bruker (^{1}H).

The oxidation protocol was adapted from a previous study by Araki *et al.* [36]. Ten grams of Brij 35 were mixed with TEMPO (286 mg, 1.83 mmol), NaBr (286 mg, 2.78 mmol), and 29 mL aqueous NaClO (available chlorine > 5.0%) at pH 10–11 and oxidized in water (100 mL) at room temperature for 24 h. The oxidation was quenched by adding 30 mL of ethanol, and the solution was acidified with HCl to pH < 1. After three extractions with 100 mL aliquots of CH_2Cl_2, the organic layers were combined and dried under reduced pressure, followed by dissolution in 250 mL hot ethanol. The product (8.3 g) was obtained by precipitation in a freezer overnight. The product was characterized by ^{1}H NMR (400 MHz, DMSO-d6): δ 12.60 (broad s, 1H), 4.01 (s, 2 H), 3.51 (m, 88H), 3.32 (m, 2H), 1.47 (p, J = 8 Hz, 2H), 1.24 (m, 18H), 0.85 (t, J = 8 Hz, 3H), see Appendix B for the ^{1}H NMR spectrum. The data are in agreement with literature [37]. In the ModBrij 35 spectrum we observe two distinct chemical shifts at 4.01 (R-O-**CH$_2$**-COOH) and 12.60 ppm (R-O-CH$_2$-COO**H**) corresponding to the headgroup of ModBrij 35, which are absent in the Brij 35 spectrum. We compute a conversion of ((1.9/3)/(2/3))* 100 % = 95 % from a comparison of the integrals of the headgroup protons at δ = 4.01 ppm (unique to ModBrij 35) to the methyl protons of the tail at δ = 0.85 ppm. Thus, 95% of the final product after purification consists of ModBrij 35.

ModBrij 35 was dispersed for 1 hr in ultrapure water to give a 25 mM stock solution. Each sample was adjusted to the desired salt concentration using NaCl, the pH was tuned using NaOH or HCl and the sample was diluted with ultrapure water to a final concentration of 10 mM ModBrij 35. After 20 min of equilibration, samples were filtered through VWR International® PTFE syringe filters with 200 nm pores. Dynamic light scattering (DLS) measurements were performed on an ALV Compact Goniometer System (CGS-3) instrument equipped with an ALV-7004 Digital Multiple Tau Real Time Correlator and a 532 nm solid state laser (40 mW). Scattering data were recorded at 90° in nine runs for each sample condition, in duplo. AfterALV software (Dullware Inc.) based on the CONTIN algorithm was used to obtain the decay rate (Γ) from the raw data. The scattering wave vector (q) and apparent diffusion coefficient (D^{app}) were computed from $q = 4\pi n_s \sin(\theta/2)/\lambda$ and $D^{app} = \Gamma/q^2$, using the refractive index (n_s), scattering angle (θ) and wavelength (λ). The apparent hydrodynamic radius (R_h) was obtained using the Stokes-Einstein equation: $D = k_B T/6\pi\eta R_h$, containing the Boltzmann constant (k_B), temperature (T) and viscosity (η). All size distributions were found to be monomodal. For simplicity, the ModBrij 35 concentration is fixed at 10 mM, whilst varying the NaCl concentration (6, 15, 28, 47 and 66 mM) and pH (from 2 to 10). We note that this means that the experimental hydrodynamic dimensions

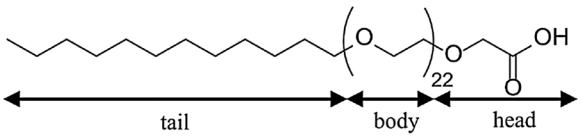

Fig. 1. Molecular structure of glycolic acid ethoxylate lauryl ether surfactant (GAELE, or ModBrij 35) and its building blocks with distinctly different solubility (tail, body, head).

reported herein are apparent sizes, as repulsive micelle-micelle interactions are not negligible at 5 and 10 mM ModBrij 35. This is reflected in a decrease in R_h with increasing surfactant concentration (see Results section).

2.2. Theory

The self-consistent mean-field (SCF) theory following the lattice discretization scheme by Scheutjens and Fleer [38,39] is a powerful tool for predicting polymer self-assembly [2,26,27,40,41]. The workhorse of theoretically studying micelle self-assembly via SCF is the so-called grand-potential (Ω) which is associated with inhomogeneities in the system. It is based upon regular solution theory, and here we apply standard first-order Markov chain statistics for the conformations of the surfactant chains. The amounts of all compounds in solution, the definition of the types of chemical units and their contact interactions are input parameters for the self-consistent minimization of the energy of the system. The set of interaction parameters is based upon previous research using the molecular SCF approach [8,42–44,26,27] (details can be found in the Appendix).

When considering charges in the system, not only contact energies between different groups but also electrostatic interactions play a role. The range of such electrostatic interactions is affected by the ionic strength (I) of the solvent, that includes both the pH and the salt concentration of the bulk solution (in the absence of surfactants). The Debye length (λ_D) is used frequently in colloidal science to express the range of electrostatic interactions [45]: every λ_D, the electrostatic repulsion decays a factor $1/e$. For water solutions at room temperature, $\lambda_D[\text{nm}] \approx 0.304/\sqrt{I[M]}$ is frequently used.

Using the thermodynamics of small systems approach [46], the grand potential energy (Ω) for micelle formation from the SCF computations provides a pathway to obtain the properties of micelles in thermodynamic equilibrium [42,43]. Such connection has been presented both for charged [44,26,27] and uncharged polymers [41]: a thermodynamically stable micelle is possible when the slope of the grand potential energy (Ω) as a function of the aggregation number (number of surfactants per micelle, g_p) decreases ($\partial\Omega/\partial g_p < 0$). When the grand potential also becomes zero, the micelle is in equilibrium with the surfactants in the bulk (at a volume fraction ϕ_p^{cmc}). This implies that the chemical potential for the surfactants in the bulk of the solution and those in the micelle are equal. Hence, for (relatively) small values of the critical micelle concentration (cmc) the chemical potential can be quantified via $\mu \approx -k_B T \ln \phi_p^{cmc}$.

Due to the symmetry of equilibrium micelles, we consider only concentration gradients in one dimension. Furthermore, even though different lattice geometries with a single gradient can be considered, we focus here on spherical lattices in which a spherical micelle can be studied. Experimentally, spherical micelles were observed for the system of interest.

3. Results and discussion

We present first the extreme cases for the acid group present in the surfactants: at low pH and at high pH. The ModBrij 35 recovers in these extremes the behaviour of non-ionic (low pH) and ionic (high pH) surfactants. Using SCF calculations, the grand potential (Ω) as a function of the number of surfactants in the spherical micelle (g_p) can be calculated (Fig. 2). Before the first stable micelle forms ($g_p \approx 18$ for pH = 2, and $g_p \approx 14$ for pH = 10), $\Omega = 0$ with increasing the *total* concentration of surfactant in the system (not shown). This indicates that at concentrations below the cmc, there is no energy penalty for the surfactants in solution (surfactant homogeneously distributed in solution). In the right panel, the surfactant bulk concentration (ϕ^{bulk}) with increasing g_p is plotted. The relatively high value of the surfactant bulk concentration indicates a high value of the cmc, and also reflects the relatively low energy penalty for surfactants in solution even when thermodynamically stable micelles are present. Equivalently, the thermodynamically stable micelles coexist with a relatively high surfactant concentration in solution. At the most stable micelle conditions, $\phi_p^{bulk} = \phi_p^{cmc}$ (with ϕ_p^{bulk} the unimer concentration in bulk). The lower the ϕ_p^{cmc} value, the stronger the tendency of surfactants to associate: hence micelle formation is more favourable at pH = 2 than at pH = 10. Note that typical SCF self-assembly studies focus on cases where the surfactants do not have such an affinity for the solvent (even when considering charged polymers): $\phi_p^{bulk} \lesssim 10^{-4}$ [43,41].

The SCF approach also provides the radial concentration profiles, from which insights about the experimentally observed trends can be extracted. Once a stable spherical micelle is obtained at given solvent conditions ($\Omega = 0$ with $\partial\Omega/\partial g_p < 0$), the SCF-predicted hydrodynamic radius (R_h^{SCF}) can be calculated from the concentration profile within the micelle [47] (see Appendix). The radial concentration profiles corresponding to $\Omega = 0$ in Fig. 2 are shown in Fig. 3, considering that r is the distance from the center of the spherical micelle. The size of the micelle at pH = 2 is larger than at pH = 10: due to the electrostatic repulsion between the charged carboxylic groups, less surfactants can be packed within a spherical geometry. Hence, both g_p and R_h^{SCF} decrease with increasing pH [43] (see cartoons in the bottom panels of Fig. 3). The difference between the outer layer of the surfactant micelle ($\approx R_h^{SCF}$) and the position of the carboxylic acid group ($\approx \text{COOH}_{Max}$, or COO^-_{Max}) gets smaller as the acid is more deprotonated (increasing pH): energy is minimized by charge screening, optimized when charges are in contact with the solvent. Furthermore, the surfactant is more concentrated in the center of the micelle at higher pH, as can be appreciated from the ordinate values at $r = 0$ (top panels). The

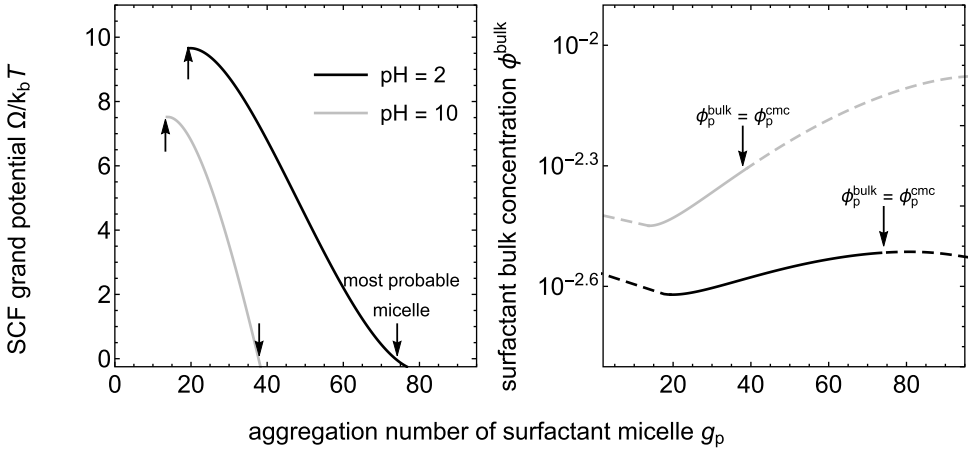

Fig. 2. Left panel: grand-potential Ω as a function of aggregation number (g_p) in aqueous salt solution with 26 mM of bulk mono-valent salt concentration at pH = 2 (black curve) and pH = 10 (gray curve). Right panel: bulk concentration of surfactant as a function of g_p. Solid curves correspond to the interval where thermodynamically stable micelles are found.

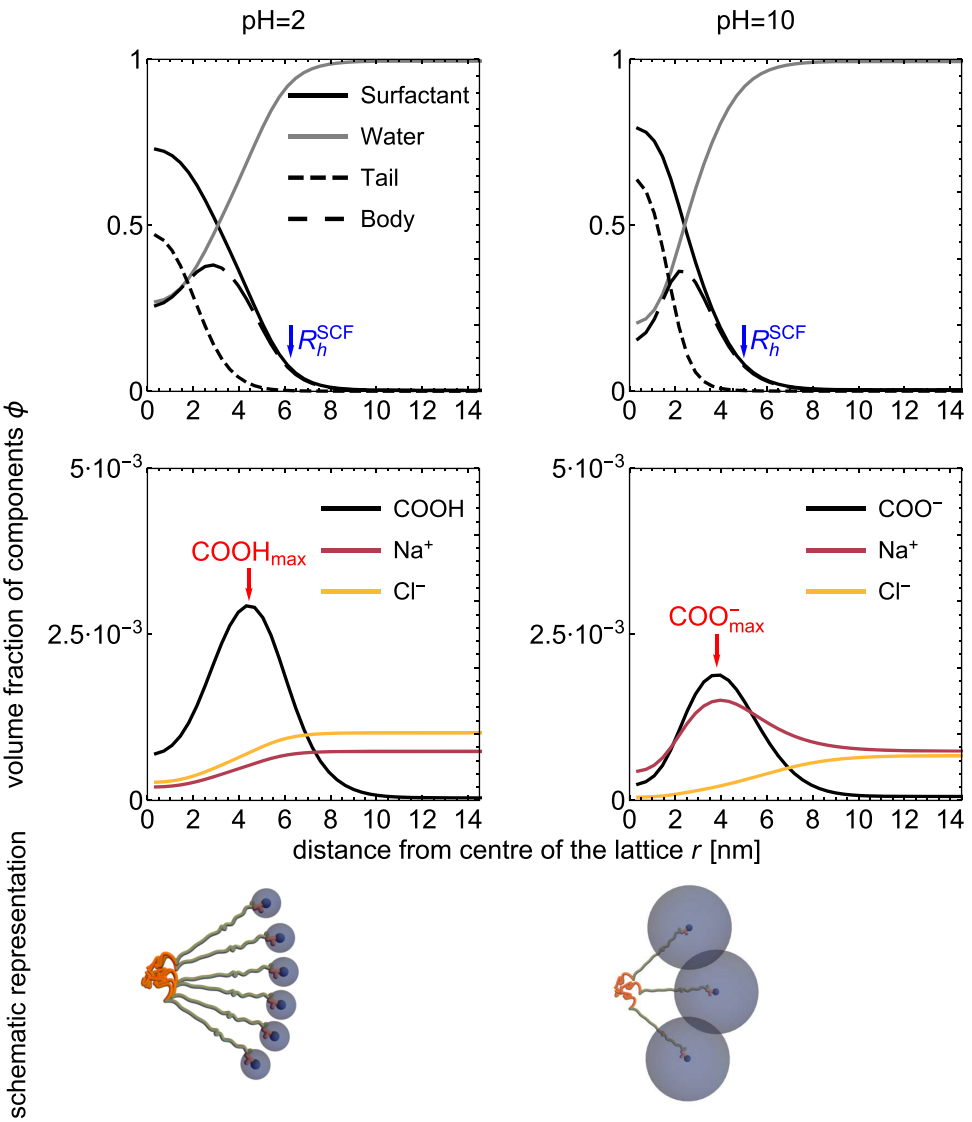

Fig. 3. Top panels: concentration profiles of surfactant (black curves) and water (gray curves) from the centre of the spherical micelle for a bulk monovalent salt concentration of 26 mM and pH = 2 (left panel) and pH = 10 (right panel). The contributions from the hydrophobic tail and the hydrophilic body of the surfactant are shown as short-dashed and long-dashed curves, respectively. Middle panels: concentration profiles of the acid groups and the dissociated monovalent salt. Bottom panels: cartoon representation of the different states (orange = tail, green = body, blue = carboxyl group and their range of repulsion). The calculated hydrodynamic radius of the micelle (blue) and the maximum concentration of carboxylic acid (red) are also shown.

configurational change of the charged groups in the surfactants when acidic groups are fully charged (pH = 10) induces a more heterogeneous distribution of the salt ions in the lattice corona with respect to the partially charged case (pH = 2). At high pH, counter ions accumulate around the charged group of the surfactants (in the corona of the micelle) as expected (see bottom panels of Fig. 3). In spite of the presence of counter-ions, a significant negative electrostatic potential profile is still observed for $r > R_h$ (see Appendix A).

The different configurations of the surfactants within the micelle are a consequence of a change in their hydrophobicity: the more charged the acid group is, the more hydrophilic the surfactant gets. This change in amphiphilicity due to a weakly-single charged group can be further

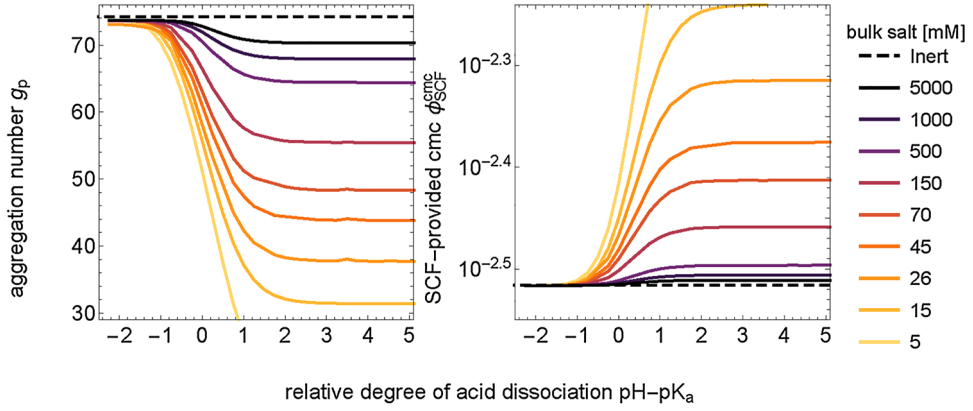

Fig. 4. Aggregation number (left) and critical micelle concentration (right) from SCF computations as a function of pH for salt concentrations ranging from 5 to 5000 mM as indicated. The straight broken lines in both plots labeled as 'inert' correspond to an SCF calculation on uncharged ModBrij 35.

studied via the critical micelle concentration (cmc) of the surfactant in solution (Fig. 4, right panel). The results in Fig. 4 are represented as a function of the difference pH − pK_a. For pH − $pK_a \ll 0$ the acid group is protonated, hence the surfactant is uncharged. pH − $pK_a \gg 0$ corresponds to a deprotonated state and thus the ModBrij 35 is negatively charged. As inferred from Fig. 4, the cmc increases with increasing pH and decreasing salt concentration (hence also the concentration of surfactant in solution coexisting with the most stable micelle). Thus, the larger the Debye length (the smaller the ionic strength), the more effectively hydrophilic the surfactant gets, and less surfactants can be packed within the micelle (Fig. 4, left panel). For small Debye lengths the partially charged acid groups are so close to each other that the interaction between surfactants is purely due to short-ranged interactions, which leads to a larger micelle ($g_p \approx 75$ at low pH independently of the bulk salt concentration considered). Note that an increase of the aggregation number implies that the free energy gain for surfactants upon micelle formation is decreased. For glycolic acid ethoxylate lauryl ether surfactants with shorter hydrophilic segments and longer hydrophobic segments, previous work also revealed an increase in cmc and a decrease in aggregation number with increasing pH [32]. We find lower aggregation numbers in the fully protonated state compared to this earlier study, as expected in view of the smaller lyophobic to lyophilic balance.

Next, we focus on the experimentally measured and the theoretically predicted hydrodynamic radius of the surfactant micelles in aqueous salt solutions, presented in Fig. 5. There is a qualitative match between the theoretical predictions and the measured hydrodynamic sizes, as a systematic deviation of about 2 nm is clearly observed. Near pH ≈ pK_a, both DLS and SCF results for the hydrodynamic radius show a salt-concentration dependent decrease in the micelle size. At a finite ModBrij 35 concentration of 5 mM and a fixed NaCl concentration of 15 mM, we obtain apparent R_h at pH 2 and 10 of 4.5 nm and 3.6 nm, respectively, corresponding to a smaller yet non-negligible difference in apparent R_h.

Such a transition of the micelle size as a function of pH was also experimentally reported for a polybase in solution [5], but in this case the observed difference in micelle size is due to the presence of a single acid group. Similar trends for size changes due to charges are also observed for weak polyelectrolyte brushes [48]: charges increase the solubility of the polymers while increasing their mutual repulsion beyond pure excluded-volume effects. For the ModBrij 35 surfactant, the combination of SCF calculations with experimental results allows distinguishing between weakly-charged micelles at low ionic strengths, whereas at high ionic strengths a strongly charged micelle is present.

By normalizing λ_D by the size of the micelle (R_h^{SCF}), we observe dissolution of the surfactants when the micelle size is of the order of the λ_D ($\lambda_D/R_h \approx 1$, Fig. 6). Once this situation is retained, the electrostatic interactions become too strong to maintain the surfactants packed into a spherical geometry: the solution limit has been reached, and the micelle falls apart into surfactants for low salt concentrations at high pH values. In essence, the unimer state is retained at conditions where the long-ranged electrostatic repulsions suppress the solvent-driven forces for micelle formation.

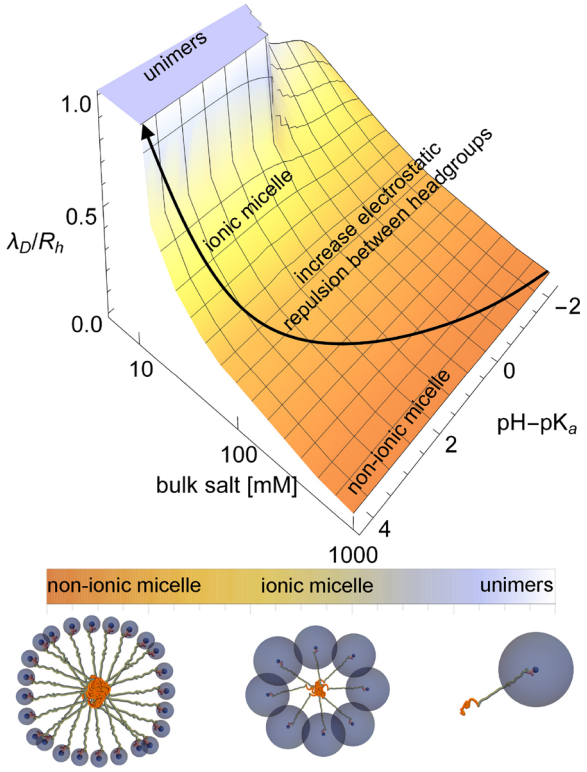

Fig. 6. State diagram of the ModBrij 35 surfactant in solution in terms of the Debye length (λ_D) normalized by the micellar hydrodynamic radius at different bulk salt concentrations and pH conditions. Cartoons represent the different surfactant states: orange segments are the hydrophobic tails, green segments the body, and blue discs represent the electrostatic interaction between the head-groups. A strong enough Coulumbic repulsion between the head groups drives the unimeric state at sufficiently high pH and low salt concentrations.

Finally, we compare the maximal difference in hydrodynamic radii observed experimentally and in the SCF computations. Thus, we consider the limiting values at pH = 2 and pH = 10 and we calculate the size difference as a function of bulk background salt (Fig. 7). We observe an exponential decay of the SCF-predicted size difference with increasing background salt. As commented previously, a higher salt concentration leads to an increase of the screening of the interaction

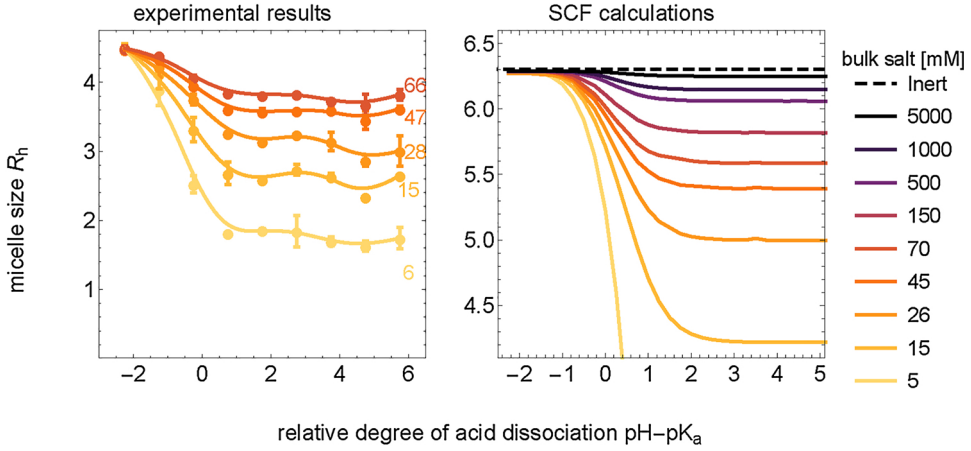

Fig. 5. DLS (left panel) and SCF (right panel) results for the hydrodynamic radius of the surfactant micelle as a function of pH at different background salt concentrations (as indicated). Experimental curves correspond to 6, 15, 28, 47 and 66 mM NaCl and SCF values range from 5 to 5000 mM. The straight broken line labeled as 'inert' corresponds to an SCF calculation on uncharged ModBrij 35.

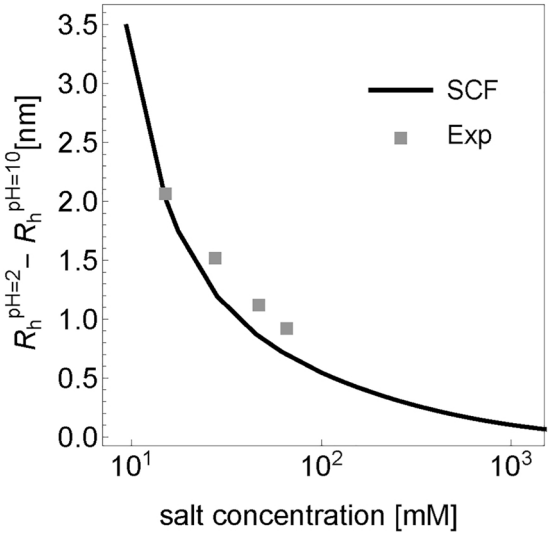

Fig. 7. Difference in hydrodynamic radius at low (pH = 2, pH − pK_a = −2.25) and high (pH = 10, pH − pK_a = 5.75) pH as a function of background mono-valent salt concentration. Gray squares correspond to experimental results, while the black curve to SCF predictions.

between the charges. This leads to a more subtle change in the micelle size. At extremely low salt concentrations, the asymptotic behavior connects once again with the solution limit. Fig. 7 shows a qualitative match between the size difference observed experimentally and the difference computed by SCF. This match is in line with findings for the absolute size as shown in Fig. 5. We note that, as experimentally most but not all surfactants are charged, the experimental unimer state may be more complex than predicted using SCF. Possibly, charged surfactants may coexist with micelles containing both charged and uncharged surfactants.

4. Conclusions

In this study we showed that the size of spherical micelles composed of surfactants with a single charge depends on the background salt concentration as well as on the pH. The SCF calculations performed are aligned with the experimentally observed trends. SCF predicts both a change in micelle size expressed via the hydrodynamic radius R_h and the limit of micelle stability. The difference in micelle size depends both on the degree of dissociation of the acid groups (set by pH − pK_a) and on the extent of screening of the electrostatic interactions (set by λ_D).

One weakly-single charged group per surfactant is enough to tune the preferred curvature of a spherical micelle using ionic strength and/or pH. At high ionic strength, the behaviour of the micelle resembles that of micelles comprising non-ionic surfactants (the head groups behave as if neutral). At intermediate ionic strength ($R_h \gg \lambda_D$) the size of the micelle remains similar to that of a non-ionic surfactant (the head groups behave as if neutral). At intermediate ionic strength ($R_h \gtrsim \lambda_D$), a change in size is observed within a certain pH interval: $-1 \lesssim$ pH − $pK_a \lesssim 1$. For low ionic strength ($R_h \lesssim \lambda_D$), the charged surfactants prefer to dissolve in water (the interactions are too strong for surfactants to reside at a curved interface). These behavioural trends (resembling micellization of uncharged amphiphiles, pH- and salt-responsive micellization, micelle dissolution) are expected to also hold for other low molar mass amphiphilic, weakly-single charged surfactants.

In conclusion, the present work reveals how SCF calculations help to qualitatively explain the self-assembly of low molar mass, weakly-charged surfactants carrying a single charge. This class of tunable surfactants are potentially suitable for many applications due to their high solubility in hard water, high salinity, and acidic as well as alkaline conditions [32].

Acknowledgements

The authors thank Dr. Feng Li, Prof. Frans Leermakers, and Gerard Krooshof for many useful comments regarding the molecular-SCF approach. We thank Dylan Atkins for the oxidation procedure of the surfactant, and Prof. Albert P. Philipse and Dr. Rodrigo Magaña Rodríguez for fruitful discussions. The Netherlands Organization for Scientific Research (NWO TA Grant No. 731.015.025) is gratefully acknowledged for financial support. Additionally, we acknowledge DSM Coating Resins and SymoChem for support.

Appendix A. Further details of the SCF computations

All SCF computations were conducted using the SFbox software, hold by F.A.M. Leermakers at Wageningen University, the Netherlands. In this work, each subunit within a molecule is assumed to occupy a single lattice unit. This implies that ModBrij 35 is modeled as a linear polymer chain containing 81 segments: (C)12((O)1(C)2)22(O)1(C)1(COOH)1. The molecule is sequestered into subunits 'C' (CH_3 or CH_2), 'O' (O) and 'COOH' (COOH). See Table A.1 for an overview of the components in the system and the short-range interactions between them, modeled via Flory–Huggins χ_{ij} parameters (with subindices $\{i, j\}$ running over all components considered).

The mono-valent salt is modelled with the same short-range interactions as the solvent (water), and the counter-ion bulk concentration (Na^+_{bulk}) is fixed. In the SCF approach, electroneutrality of the bulk solution is ensured. In the presence of water, the carboxylic acid dissociates: $COOH + H_2O \rightleftarrows COO^- + H_3O^+$. The equilibrium is described by a dissociation constant (K_a), which we set as $pK_a = 4.25$. In accordance with experimental data from the literature, $pK_a = 4.25$ [32]. The pK_a was defined within SCF following [27], wherein further details on SCF computations with carboxylic groups can be found. In order to define electrostatic interactions, the lattice size needs be defined. In this work, the lattice size is set to 0.36 nm. This lattice size leads to an effective value due to the lattice-to-real units conversion of $pK_a^{lat} = 5.8$. For the water dissociation constant ($pK_W = 14$), $pK_W^{lat} = 17.1$.

The SCF-generated protonation curve is presented in Fig. A.8. Note that the charge per surfactant does not depend on the background counter-ion concentration, but only on the relative pH considered (pH − pK_a). For negative pH − pK_a values, the carboxylic acid groups are only weakly negatively charged. On the contrary, when pH ≫ pK_a, the acid group gets deprotonated as expected. Note that the condition from weak-charge to

Table A.1
Set of Flory–Huggins χ parameters employed to model aqueous ModBrij 35 solutions.

Component	C	O	COOH	H_2O
C	0	1	1.6	1.6
O	1	0	−0.7	−0.7
COOH	1.6	−0.7	0	0
H_2O	1.6	−0.7	0	0

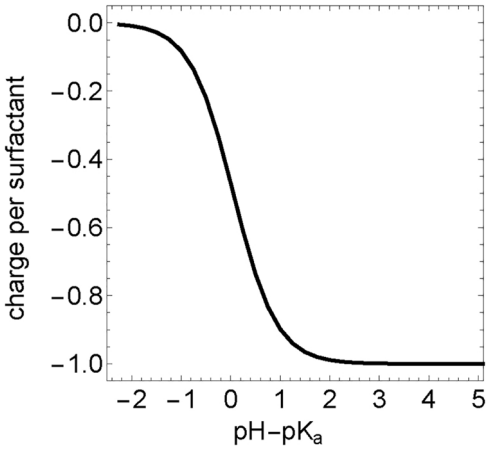

Fig. A.8. Charge per surfactant as a function of pH (SCF-like protonation curve). This curve does not depend on the salt concentration, but only on the pH and PK_a values, which are the same in all calculations conducted.

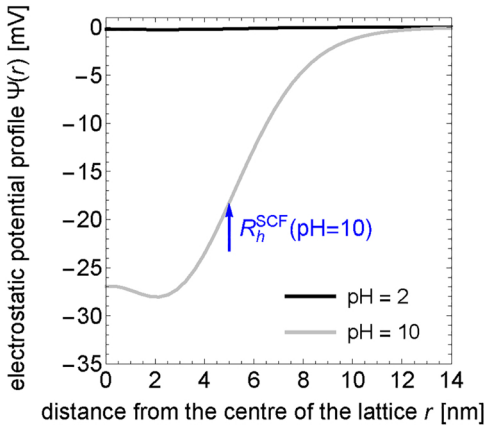

Fig. A.9. Radial electrostatic potential profile from the centre of a spherical micelle (corresponding to profiles in Fig. 3) for a bulk monovalent salt concentration of 26 mM and pH = 2 and pH = 10 as indicated.

completely charge spans over about 4 pH values (−2 to 2). We also report here the radial electrostatic potential profile as provided from the SCF calculations in Fig. A.9. This plot shows an overall negative electrostatic potential for $r > R_h$ at sufficiently high pH and low salt concentrations.

For the calculation of the hydrodynamic micelle radius from the radial concentration profiles we follow the method in [47,49]. In essence, one relates the (theoretical) relative solvent velocity profile to the polymer radial concentration profile. At each layer r, the quantity $\alpha(r)$ relates to the concentration profile of the surfactant (ϕ_p):

$$\alpha(r) = \frac{q(r)\tanh q^{-1}(r) + \alpha(r-1)}{1 + \alpha(r-1)q^{-1}(r)\tanh q^{-1}(r)}, \tag{A.1}$$

where the auxiliary function $q(r)$ is the surfactant concentration w.r.t. the bulk:

$$\begin{aligned} q(r) &= \sqrt{\frac{1-\Delta\phi_p(r)}{\Delta\phi_p(r)}} \\ \Delta\phi_p(r) &= \phi_p(r) - \phi_p^{bulk} \end{aligned} \tag{A.2}$$

Following this method, the hydrodynamic size R_h^{SCF} is the lattice layer at which the relative solvent velocity remains constant:

$$R_h^{SCF} = r - \alpha(r), \tag{A.3}$$

subject to the convergence criteria $\alpha(r) - \alpha(r-1) = 1$ (the hydrodynamic size is defined when $r - \alpha(r)$ is constant).

Appendix B. NMR analysis

In this section, we confirm the functionalization of Brij 35 which provides a carboxylic acid head group. To evaluate the conversion of Brij 35 (Fig. B.10, top left) into ModBrij 35 (Fig. B.10, top right), we performed ^{1}H NMR spectroscopy on both compounds (Fig. B.10 bottom panel). In the ModBrij 35 spectrum we observe two distinct chemical shifts, which are absent in the Brij 35 spectrum and correspond to the protons of the carboxylic acid headgroup, R-O-CH_2-COO**H** at δ = 12.60 ppm and R-O-**CH_2**-COOH at δ = 4.01 ppm. Note that the headgroup protons of unmodified Brij 35 are observed at δ = 3.68 and δ = 4.55 ppm in both spectra (albeit much more pronounced in the Brij 35 spectrum) as full conversion is not achieved.

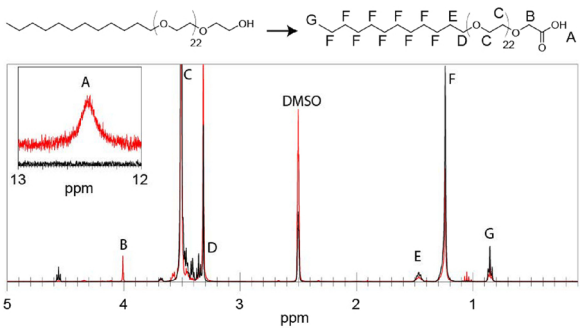

Fig. B.10. ^{1}H NMR of unmodified Brij 35 (top left, black) and ModBrij 35 (top right, red) (400 MHz, DMSO-d6): δ 12.60 (broad s, 1H), 4.01 (s, 2H), 3.51 (m, 88H), 3.32 (m, 2H), 1.47 (p, J = 8 Hz, 2H), 1.24 (m, 18H), 0.85 (t, J = 8 Hz, 3H). The conversion is computed from the ratio of the integrals of protons B and G, which gives a conversion of 95%.

References

[1] Y.S. Lee, K.W. Woo, Micellization of aqueous cationic surfactant solutions at the micellar structure transition concentration-based upon the concept of the pseudo-phase separation, J. Colloid Interface Sci. 169 (1) (1995) 34–38.

[2] E.B. Zhulina, O.V. Borisov, Theory of block polymer micelles: recent advances and current challenges, Macromolecules 45 (11) (2012) 4429–4440.

[3] F.A.M. Leermakers, P.J. Atkinson, E. Dickinson, D.S. Horne, Self-consistent-field modeling of adsorbed β-casein: effects of pH and ionic strength on surface coverage and density profile, J. Colloid Interface Sci. 178 (2) (1996) 681–693.

[4] E.B. Zhulina, O.V. Borisov, Self-assembly in solution of block copolymers with annealing polyelectrolyte blocks, Macromolecules 35 (24) (2002) 9191–9203.

[5] L. Xu, Z. Zhu, O.V. Borisov, E.B. Zhulina, S.A. Sukhishvili, pH-triggered block copolymer micelle-to-micelle phase transition, Phys. Rev. Lett. 103 (11) (2009) 118301.

[6] A. Heindl, H.-H. Kohler, Rod formation of ionic surfactants: a thermodynamic model, Langmuir 12 (10) (1996) 2464–2477.

[7] K. Thalberg, B. Lindman, K. Bergfeldt, Phase behavior of systems of polyacrylate and cationic surfactants, Langmuir 7 (12) (1991) 2893–2898.

[8] M.R. Böhmer, L.K. Koopal, J. Lyklema, Micellization of ionic surfactants: calculations based on a self-consistent field lattice model, Journal of Physical Chemistry 95 (23) (1991) 9569–9578.

[9] A. Chatterjee, S.P. Moulik, S.K. Sanyal, B.K. Mishra, P.M. Puri, Thermodynamics of micelle formation of ionic surfactants: a critical assessment for sodium dodecyl sulfate, cetyl pyridinium chloride and dioctyl sulfosuccinate (Na salt) by microcalorimetric, conductometric, and tensiometric measurements, Journal of Physical Chemistry B 105 (51) (2001) 12823–12831.

[10] A. Dobrynin, M. Rubinstein, Theory of polyelectrolytes in solutions and at surfaces, Prog. Polym. Sci. 30 (11) (2005) 1049–1118.

[11] N. Gorski, M. Gradzielski, H. Hoffmann, Mixtures of nonionic and ionic surfactants. The effect of counterion binding in mixtures of tetradecyldimethylamine oxide and tetradecyltrimethylammonium bromide, Langmuir 10 (8) (1994) 2594–2603.

[12] O. Söderman, K.L. Herrington, E.W. Kaler, D.D. Miller, Transition from micelles to vesicles in aqueous mixtures of anionic and cationic surfactants, Langmuir 13 (21) (1997) 5531–5538.

[13] D.E. Jennings, Y.A. Kuznetsov, E.G. Timoshenko, K.A. Dawson, Conformational transitions in a lattice model of a three-component mixture of solvent, amphiphile, and soluble polymers, J. Chem. Phys. 108 (4) (1998) 1702–1709.

[14] A.J. Konop, R.H. Colby, Role of condensed counterions in the thermodynamics of surfactant micelle formation with and without oppositely charged polyelectrolytes, Langmuir 15 (1) (1999) 58–65.

[15] T. Wallin, P. Linse, Polyelectrolyte-induced micellization of charged surfactants. Calculations based on a self-consistent field lattice model, Langmuir 14 (11) (1998) 2940–2949.

[16] E.F. Marques, O. Regev, A. Khan, M. da Graca Miguel, B. Lindman, Vesicle formation and general phase behavior in the catanionic mixture SDS-DDAB-water. The anionic-rich side, J. Phys. Chem. B 102 (35) (1998) 6746–6758.

[17] L. Vitorazi, J.-F. Berret, W. Loh, Self-assembly of complex salts of cationic surfactants and anionic-neutral block copolymers. Dispersions with liquid-crystalline internal structure, Langmuir 29 (46) (2013) 14024–14033.

[18] P. Linse, Micellization of poly (ethylene oxide)-poly (propylene oxide) block copolymers in aqueous solution: effect of polymer polydispersity, Macromolecules 27 (22) (1994) 6404–6417.

[19] Fluorescence Studies of Polymer Containing Systems, in: K. Procházka (Ed.), Springer Series on Fluorescence, vol. 16, Springer International Publishing, 2016.

[20] Z.A. Al-Anber, The thermodynamics of micelles in surfactant solution: lattice mean field theory, Colloid J. 69 (5) (2007) 541–545.

[21] T. Wallin, P. Linse, Monte Carlo simulations of polyelectrolytes at charged micelles. 2. Effects of linear charge density, J. Phys. Chem. 100 (45) (1996) 17873–17880.

[22] T. Wallin, P. Linse, Monte Carlo simulations of polyelectrolytes at charged micelles. 3. Effects of surfactant tail length, J. Phys. Chem. B 101 (28) (1997) 5506–5513.

[23] G. Riess, Micellization of block copolymers, Prog. Polym. Sci. 28 (7) (2003) 1107–1170.

[24] A.H.E. Müller, O. Borisov (Eds.), Self Organized Nanostructures of Amphiphilic Block Copolymers Advances in Polymer Science, vol. 241–242, Springer, Berlin, 2011.

[25] J. van der Gucht, E. Spruijt, M. Lemmers, M.A. Cohen Stuart, Polyelectrolyte complexes: bulk phases and colloidal systems, J. Colloid Interface Sci. 361 (2) (2011) 407–422.

[26] F. Li, M. Schellekens, J. de Bont, R. Peters, A. Overbeek, F.A.M. Leermakers, R. Tuinier, Self-assembled structures of PMAA-PMMA block copolymers: synthesis, characterization, and self-consistent field computations, Macromolecules 48 (4) (2015) 1194–1203.

[27] F. Li, R. Tuinier, I. van Casteren, R. Tennebroek, A. Overbeek, F.A.M. Leermakers, Self-organization of polyurethane pre-polymers as studied by self-consistent field theory, Macromol. Theory Simulat. 25 (1) (2016) 16–27.

[28] L.L. Schramm, E.N. Stasiuk, D.G. Marangoni, 2 Surfactants and their applications, Annu. Rep. Prog. Chem. Sect. C: Phys. Chem. 99 (2003) 3–48.

[29] D. Myers, Surfactant Science and Technology: Myers/Surfactant Science and Technology, 3rd ed., John Wiley & Sons, Inc., Hoboken, NJ, USA, 2005.

[30] G. Ziyatdinova, E. Ziganshina, P.N. Cong, H. Budnikov, Voltammetric determination of thymol in oregano using CeO2-modified electrode in BrijTDEQN##2## 35 micellar medium, Food Anal. Methods 10 (1) (2017) 129–136.

[31] M. Fanun, Microemulsions. Properties and Applications, Taylor & Francis, 2008.

[32] L. Chiappisi, Polyoxyethylene alkyl ether carboxylic acids: an overview of a neglected class of surfactants with multiresponsive properties, Adv. Colloid Interface Sci. 250 (2017) 79–94.

[33] T. Ozawa, K. Endo, T. Masui, M. Miyaki, K. Matsuo, S. Yamada, Advantage of sodium polyoxyethylene lauryl ether carboxylate as a mild cleansing agent, J. Surfactants Detergents 19 (4) (2015) 785–794.

[34] G.A. Jürgenson, V. Bittner, C. Kurkal-Siebert, G. Oetter, J. Tinsley, Alkyl Ether Carboxylate Surfactants for Chemically Enhanced Oil Recovery in Harsh Field Conditions, Society of Petroleum Engineers SPE-174589-MS, 2015 doi:10.2118/174589-MS.

[35] F. Fu, Q. Wang, Removal of heavy metal ions from wastewaters: a review, J. Environ. Manag. 92 (3) (2011) 407–418.

[36] J. Araki, C. Zhao, K. Ito, Efficient production of polyrotaxanes from α-cyclodextrin and poly(ethylene glycol), Macromolecules 38 (17) (2005) 7524–7527.

[37] F.-X. Gallat, A.P.S. Brogan, Y. Fichou, N. McGrath, M. Moulin, M. Härtlein, J. Combet, J. Wuttke, S. Mann, G. Zaccai, C.J. Jackson, A.W. Perriman, M. Weik, A polymer surfactant corona dynamically replaces water in solvent-free protein liquids and ensures macromolecular flexibility and activity, J. Am. Chem. Soc. 134 (32) (2012) 13168–13171.

[38] J.M.H.M. Scheutjens, G.J. Fleer, Statistical theory of the adsorption of interacting chain molecules. 1. Partition function, segment density distribution, and adsorption isotherms, J. Phys. Chem. 83 (12) (1979) 1619–1635.

[39] G.J. Fleer, M.A. Cohen Stuart, J.M.H.M. Scheutjens, T. Cosgrove, B. Vincent, Polymers at Interfaces, Springer Netherlands, 1993.

[40] A. Arora, J. Qin, D.C. Morse, K.T. Delaney, G.H. Fredrickson, F.S. Bates, K.D. Dorfman, Broadly accessible self-consistent field theory for block polymer materials discovery, Macromolecules 49 (13) (2016) 4675–4690.

[41] A. Ianiro, J. Patterson, Á. González García, M.M.J. van Rijt, M.M.R.M. Hendrix, N.A.J.M. Sommerdijk, I.K. Voets, A.C.C. Esteves, R. Tuinier, A roadmap for poly (ethylene oxide)-block-poly-ε-caprolactone self-assembly in water: prediction, synthesis, and characterization, J. Polym. Sci. Part B: Polym. Phys. 56 (4) (2017).

[42] F.A.M. Leermakers, J.C. Eriksson, J. Lyklema, Association colloids and their equilibrium modelling, Fundamentals of Interface and Colloid Science vol. 5, Elsevier, 2005 pp. 4.1–4.123.

[43] Y. Lauw, F.A.M. Leermakers, M.A. Cohen Stuart, Self-consistent-field analysis of the micellization of carboxy-modified poly(ethylene oxide)-poly(propylene oxide)-poly (ethylene oxide) triblock copolymers, J. Phys. Chem. B 110 (1) (2006) 465–477.

[44] F. Li, A.T.M. Marcelis, E.J.R. Sudhölter, M.A. Cohen Stuart, F.A.M. Leermakers, Field theoretical modeling of the coexistence of micelles and vesicles in binary copolymer mixtures, Soft Matter 5 (21) (2009) 4173.

[45] J. Riley, Charge in Colloidal Systems, Wiley-Blackwell, 2009.

[46] T.L. Hill, Thermodynamics of Small Systems. Parts I & II vol. 3, WILEY-VCH Verlag, 1965.

[47] J.M.H.M. Scheutjens, G.J. Fleer, M.A. Cohen Stuart, End effects in polymer adsorption: a tale of tails, Colloids Surf. 21 (1986) 285–306.

[48] J.D. Willott, T.J. Murdoch, F.A.M. Leermakers, W.M. de Vos, Behavior of weak polyelectrolyte brushes in mixed salt solutions, Macromolecules 51 (3) (2018) 1198–1206.

[49] M.A. Cohen Stuart, F.H.W.H. Waajen, T. Cosgrove, B. Vincent, T.L. Crowley, Hydrodynamic thickness of adsorbed polymer layers, Macromolecules 17 (9) (1984) 1825–1830.